ISSN 1749-3889 (print), 1749-3897 (online)
International Journal of Nonlinear Science
Vol.22(2016) No.3, pp.153-166

Mixed Convection Over An Inclined Wavy Surface Embedded in A Thermally Stratified Porous Medium Saturated with A Nanofluid

D.Srinivasacharya *, P. Vijay Kumar
Department of Mathematics, National Institute of Technology, Warangal-506004, Telangana, India
(Received 15 July 2015, accepted 12 October 2016)

Abstract: The objective of this article is to study the effect of thermal stratification on mixed convection in a nanofluid along an inclined wavy surface embedded in a porous medium. A coordinate transformation is employed to transform the complex wavy surface to a smooth surface. The governing equations are transformed into a set of partial differential equations using the non-similarity transformation and then applied the local similarity and non-similarity method to obtain coupled ordinary differential equations. Now, these equations are solved using the successive linearization method. The present results are compared with previously published work and are found to be in very good agreement. The effects of thermal stratification parameter, Brownian motion parameter, thermophoresis parameter, amplitude of the wavy surface, angle of inclination of the wavy surface on the non-dimensional velocity, temperature, nanoparticle volume fraction, heat and nanoparticle mass transfer rates for both aiding and opposing flows are studied and displayed graphically.

Keywords: Mixed convection; Nanofluid; inclined wavy surface; Thermal stratification; Porous medium; Brownian motion; Thermophoresis.

1 Introduction

Conventional heat transfer fluids such as water, oil or ethylene glycol have low thermal conductivity which leads to low heat transfer performance. So, to improve the heat transfer performance, Choi [1] added a small amount (less than 1% by volume) of metallic nanoparticles in to these conventional heat transfer fluids so called nanofluids. Furthermore, few experiments have shown that some nanofluids enhance the convective heat transfer coefficient by up to 100% compared to that of water [2, 3]. Nanofluids are used in many applications in heat transfer including microelectronics, fuel cells, pharmaceutical processes and hybrid-powered engines [4]. Besides this, Nanofluids also have several engineering applications such as microfluidics, transportation, biomedical, solid-state lighting, manufacturing, high-power X-rays, scientific measurement, material processing, medicine and material synthesis. A detailed review on nanofluids can be found in the book by Das *et al.*[5] and collection of literature by Kakac and Pramuanjaroenkij [6] and Gianluca *et al.*[7]

Mixed convection heat transfer flow in porous media has been widely studied in recent years due to its wide range of engineering applications such as chemical processing equipment, electronic device cooling, lubrication systems, solar energy collectors, food processing, heat exchangers, geothermal and hydrocarbon recovery and so on. An indepth review of convective heat transfer in porous medium is presented in the book by Nield and Bejan [8]. Mirmasoumi and Behzadmehr [9] investigated the effect of nanoparticles mean diameter on mixed convection heat transfer of a nanofluid in a horizontal tube. They have reported that the convection heat transfer coefficient enhances with decreasing nanoparticle mean diameter. Cho *et al.* [10] examined the mixed convection heat transfer characteristics of water based nanofluids in lid driven cavity with wavy surfaces. Rasekh and Ganji [11] analytically studied the problem of mixed convection heat transfer of a steady state boundary layer flow about an inclined plate in a porous medium filled with nanofluid.

Thermal stratification on convection in a fluid saturated porous medium is widely accepted due to its geophysical and industrial applications such as hot dike complexes in volcanic regions for heating of ground water, development of advanced technologies for nuclear waste management, pollutant and contaminant transport in soil etc. Generally,

*Corresponding author. *E-mail address*: dsrinivasacharya@yahoo.com, dsc@nitw.ac.in

IJNS.2016.12.15/936

stratification of fluid arises due to the temperature variations, concentration differences or the presence of different fluids. Ishak *et al.* [12] theoretically studied the similarity solutions of the mixed convection boundary layer flow over a vertical surface embedded in a thermally stratified porous medium. They have reported that the thermal stratification significantly affects the surface heat transfer as well as surface shear stress. Bansod and Jadhav [13] studied the effect of double stratification on mixed convection heat and mass transfer from a vertical surface in a fluid saturated porous medium. Ibrahim and Makinde [14] presented a boundary layer analysis for free convection flow in a doubly stratified nanofluid over a vertical plate with uniform surface and mass flux conditions. Mahmoud and Waheed [15] investigated the problem of steady two dimensional mixed convection flow of a micropolar fluid over stretching permeable vertical surface with radiation and thermal stratification effects. They have shown that the local Nusselt number and wall couple stress decrease with increasing thermal stratification parmeter. Arifin *et al.* [16] performed a numerical investigation of the steady mixed convection boundary layer flow over a vertical surface embedded in a thermally stratified porous medium saturated by a nanofluid. Shezad *et al.* [17] studied the mixed convection flow of a thixotropic fluid with thermal stratification and thermal radiation effects and showed that the thermal stratification effect corresponds to small values of local Nusselt number, when compared with case of no thermal stratification effects. Srinivasacharya and Surender [18] investigated the effect of thermal and mass stratification on mixed convection boundary layer flow of a nanofluid saturated porous medium. Rashad *et al.* [19] studied mixed convection flow of a micropolar fluid on a vertical flat plate immersed in thermally and solutally stratified medium with chemical reaction.

The study of heat and mass transfer from the irregular wavy surfaces is of fundamental importance because of its enhancing heat transfer characteristics. Irregularities in surfaces occur in many practical situations. These irregularities encounter in several heat transfer devices such as microelectronic devices, flat plate solar collectors and flat plate condensers in refrigerators. The preceding literature reveals that the problem of mixed convection over an inclined wavy surface embedded in a thermally stratified porous medium saturated with nanofluid has not been considered so far. The present study mainly focussed on exploring the effects of thermal stratification, Brownian motion, thermoporesis, amplitude and angle of inclination of the wavy plate on mixed convection in Darcy porous medium saturated with nanofluid.

2 Mathematical formulation

Consider the steady laminar incompressible two-dimensional boundary layer mixed convection flow along a semi-infinite inclined wavy surface embedded in a nanofluid saturated Darcy porous medium. The wavy plate is inclined at an angle A ($0^o \leq A \leq 90^o$) to the horizontal. The inclination angle is 0^o (for horizontal plate), 90^o (for vertical plate) and $0^o < A < 90^o$ (for inclined plate). The coordinate system is shown in Fig.1. The wavy surface is described by

$$y = \delta(x) = a\sin(\pi x/l)$$

where a is the amplitude of the wavy surface, and $2l$ is the characteristic length of the wavy surface. The wavy surface is held at constant temperature T_w and constant nanoparticle volume fraction ϕ_w and the ambient medium is assumed to be linearly stratified with respect to the temperature in the form $T_\infty(x) = T_{\infty,0} + Bx$ where B is a constant varied to alter the intensity of stratification in the medium. The values of T_w and ϕ_w are assumed to be greater than the porous medium temperature $T_{\infty,0}$ and nanoparticle volume fraction ϕ_∞ sufficiently far from the wavy surface.

The porous medium is considered to be homogeneous and isotropic and is saturated with a fluid which is in local thermodynamic equilibrium with the solid matrix. The fluid has constant properties except the density in the buoyancy term of the balance of momentum equation. The governing equations for this problem under the laminar boundary layer flow assumptions, Boussinesq approximation and using the Darcy's flow through a homogeneous porous medium near the inclined wavy surface are given by

$$\frac{\partial u}{\partial x} + \frac{\partial v}{\partial y} = 0 \tag{1}$$

$$\frac{\partial u}{\partial y} - \frac{\partial v}{\partial x} = \frac{(1-\phi_\infty)\rho_{f_\infty}\beta\, K\, g}{\mu}\left(\frac{\partial T}{\partial y}\sin A - \frac{\partial T}{\partial x}\cos A\right) - \frac{(\rho_p - \rho_{f_\infty})\, K\, g}{\mu}\left(\frac{\partial \phi}{\partial y}\sin A - \frac{\partial \phi}{\partial x}\cos A\right) \tag{2}$$

$$u\frac{\partial T}{\partial x} + v\frac{\partial T}{\partial y} = \alpha\left(\frac{\partial^2 T}{\partial x^2} + \frac{\partial^2 T}{\partial y^2}\right) + \gamma\left[D_B\left(\frac{\partial \phi}{\partial x}\frac{\partial T}{\partial x} + \frac{\partial \phi}{\partial y}\frac{\partial T}{\partial y}\right) + \frac{D_T}{T_\infty}\left(\left(\frac{\partial T}{\partial x}\right)^2 + \left(\frac{\partial T}{\partial y}\right)^2\right)\right] \tag{3}$$

$$u\frac{\partial \phi}{\partial x} + v\frac{\partial \phi}{\partial y} = D_B\left(\frac{\partial^2 \phi}{\partial x^2} + \frac{\partial^2 \phi}{\partial y^2}\right) + \frac{D_T}{T_\infty}\left(\frac{\partial^2 T}{\partial x^2} + \frac{\partial^2 T}{\partial y^2}\right) \tag{4}$$

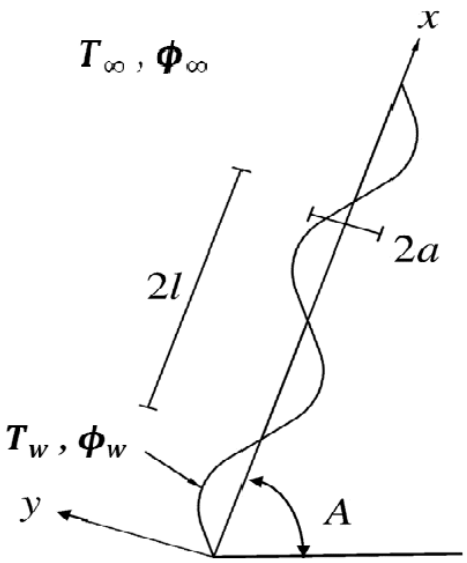

Figure 1: Physical model

where u and v are the Darcy velocity components in the x and y directions, respectively, T is the temperature, ϕ is the nanoparticle concentration, g is the acceleration due to gravity, K is the permeability, ρ_f is the the density of the base fluid, ρ_p is the density of the particles, α is the effective thermal diffusivity, β is the volumetric thermal expansion coefficient of the nanofluid, μ is the dynamic viscosity of the fluid, D_B is the Brownian diffusion coefficient, D_T is the thermophoretic diffusion coefficient and γ is the ratio between the effective heat capacity of the nanoparticle material and heat capacity of the fluid. The above equations are written on the assumption that the nanosized particles are suspended in uniform distribution in a base fluid to form a nanofluid. When the nanofluid passes through porous media, the suspension of the nanoparticles is maintained using a surfactant or some surface charge technology to prevent their agglomeration and to avoid being captured by the porous matrix.

The boundary conditions are

$$v = 0, \quad T = T_w, \quad \phi = \phi_w, \quad \text{at} \quad y = \delta(x) \tag{5a}$$

$$u = U_\infty, \quad T \to T_\infty, \quad \phi \to \phi_\infty \quad \text{as} \quad y \to \infty \tag{5b}$$

Introducing the stream function ψ by

$$u = \frac{\partial \psi}{\partial y}, \quad v = -\frac{\partial \psi}{\partial x} \tag{6}$$

and the following non-dimensional variables

$$(\hat{x}, \hat{y}, \hat{a}, \hat{\delta}) = l^{-1}(x, y, a, \delta), \quad \theta = \frac{T - T_{\infty,x}}{T_w - T_\infty, 0}, \quad \hat{\psi} = \frac{\psi}{U_\infty l}, \quad s = \frac{\phi - \phi_\infty}{\phi_w - \phi_\infty} \tag{7}$$

in Eqs.(2)-(4), we get the following system of non-dimensional equations

$$\frac{\partial^2 \hat{\psi}}{\partial \hat{x}^2} + \frac{\partial^2 \hat{\psi}}{\partial \hat{y}^2} = \Delta \left[\left(\frac{\partial \theta}{\partial \hat{y}} \sin A - S_T \cos A - \frac{\partial \theta}{\partial \hat{x}} \cos A \right) - N_r \left(\frac{\partial s}{\partial \hat{y}} \sin A - \frac{\partial s}{\partial \hat{x}} \cos A \right) \right] \tag{8}$$

$$Pe \left(S_T \frac{\partial \hat{\psi}}{\partial \hat{y}} + \frac{\partial \hat{\psi}}{\partial \hat{y}} \frac{\partial \theta}{\partial \hat{x}} - \frac{\partial \hat{\psi}}{\partial \hat{x}} \frac{\partial \theta}{\partial \hat{y}} \right) = \frac{\partial^2 \theta}{\partial \hat{x}^2} + \frac{\partial^2 \theta}{\partial \hat{y}^2} + N_b \left(S_T \frac{\partial s}{\partial \hat{x}} + \frac{\partial s}{\partial \hat{x}} \frac{\partial \theta}{\partial \hat{x}} + \frac{\partial s}{\partial \hat{y}} \frac{\partial \theta}{\partial \hat{y}} \right) + N_t \left(S_T^2 + \left(\frac{\partial \theta}{\partial \hat{x}} \right)^2 + \left(\frac{\partial \theta}{\partial \hat{y}} \right)^2 + 2 S_T \frac{\partial \theta}{\partial \hat{x}} \right) \tag{9}$$

$$Pe\left(\frac{\partial\hat{\psi}}{\partial\hat{y}}\frac{\partial s}{\partial\hat{x}}-\frac{\partial\hat{\psi}}{\partial\hat{x}}\frac{\partial s}{\partial\hat{y}}\right)=\frac{1}{Le}\left[\left(\frac{\partial^2 s}{\partial\hat{x}^2}+\frac{\partial^2 s}{\partial\hat{y}^2}\right)+\frac{N_t}{N_b}\left(\frac{\partial^2\theta}{\partial\hat{x}^2}+\frac{\partial^2\theta}{\partial\hat{y}^2}\right)\right] \tag{10}$$

where $\Delta=\dfrac{Ra}{Pe}$ is the Mixed convection parameter, $Ra=\dfrac{(1-\phi_\infty)\rho_{f_\infty}\beta\,K\,g\,(T_w-T_{\infty,0})l}{\mu\alpha}$ is the Rayleigh number, $Pe=\dfrac{U_\infty l}{\alpha}$ is the Peclet number, $N_r=\dfrac{(\rho_p-\rho_{f_\infty})(\phi_w-\phi_\infty)}{\rho_{f_\infty}\beta(T_w-T_{\infty,0})(1-\phi_\infty)}$ is the buoyancy ratio, $N_b=\dfrac{\gamma D_B(\phi_w-\phi_\infty)}{\alpha}$ is the Brownian motion parameter, $N_t=\dfrac{\gamma D_T(T_w-T_{\infty,0})}{\alpha T_\infty}$ is the thermophoresis parameter, $Le=\dfrac{\alpha}{D_B}$ is the Lewis number, and $S_T=\dfrac{Bl}{T_w-T_{\infty,0}}$ is the thermal stratification parameter.

The effect of the wavy surface can be transferred from the boundary conditions into the governing equations by the coordinate transformation

$$\xi=\hat{x},\quad \eta=\frac{(\hat{y}-\delta)Pe^{1/2}}{\xi^{1/2}(1+\dot{\delta}^2)},\quad \hat{\psi}=Pe^{-1/2}\xi^{1/2}f(\xi,\eta),\quad \theta=\theta(\xi,\eta),\quad s=s(\xi,\eta) \tag{11}$$

Substituting Eq. (11) into Eqs.(8)-(10) and letting $Pe\to\infty$ (i.e., boundary layer approximation), we obtain the following equations:

$$f''=\Delta(\sin A+\dot{\delta}\cos A)\,(\theta'-N_r s') \tag{12}$$

$$\theta''+\frac{1}{2}f\theta'+N_b s'\theta'+N_t\theta'^2=\xi\left(S_T f'+f'\frac{\partial\theta}{\partial\xi}-\theta'\frac{\partial f}{\partial\xi}\right) \tag{13}$$

$$s''+\frac{1}{2}Lefs'+\frac{N_t}{N_b}\theta''=Le\xi\left(f'\frac{\partial s}{\partial\xi}-s'\frac{\partial f}{\partial\xi}\right) \tag{14}$$

The associated boundary conditions are

$$f+2\xi\left(\frac{\partial f}{\partial\xi}\right)_{\eta=0}=0,\quad \theta=1-S_T\xi,\quad s=1,\quad \text{at}\quad \eta=0 \tag{15a}$$

$$f'=1,\quad \theta\to 0,\quad s\to 0\quad \text{as}\quad \eta\to\infty, \tag{15b}$$

The primary objective of this study is to estimate the parameters of engineering interest in fluid flow, heat and nanoparticle mass transport problems, namely the Nusselt number Nu and nanoparticle Sherwood number NSh. These parameters characterize the wall heat and nanoparticle mass transfer rates, respectively.

The local heat and nanoparticle mass fluxes from the wavy plate can be obtained from

$$q_w=-kn.\nabla T,\qquad q_{np}=-D_B n.\nabla\phi \tag{16}$$

where $n=\left(\frac{-\dot{\delta}}{\sqrt{1+\dot{\delta}^2}},\frac{1}{\sqrt{1+\dot{\delta}^2}}\right)$ is the unit normal vector to the wavy plate.

The dimensionless local Nusselt number $Nu=\frac{xq_w}{k(T_w-T_\infty)}$ and the nanoparticle Sherwood number $NSh=\frac{xq_{np}}{D_B(\phi_w-\phi_\infty)}$ are given by

$$\frac{Nu_\xi}{\sqrt{Pe_\xi}}=-\frac{\theta'(\xi,0)}{(1-S_T\xi)(1+\dot{\delta}^2)^{1/2}},\qquad \frac{NSh_\xi}{\sqrt{Pe_\xi}}=-\frac{s'(\xi,0)}{(1+\dot{\delta}^2)^{1/2}}, \tag{17}$$

3 Method of Solution

To solve the system of Eqns. (12)-(14) along with the boundary conditions (15), we first apply a local similarity and non-similarity method which has been applied by the many of the researchers [20, 21] to solve various non-similar boundary value problems. The boundary value problems resulting from this method are solved by the successive linearisation method.

In the first level of truncation, the terms accompanied by $\xi\frac{\partial}{\partial\xi}$ are assumed to be very small. This is particularly true when $\xi<<1$. Thus the terms with $\xi\frac{\partial}{\partial\xi}$ in Eqns. (12)-(14) can be neglected to get the following system of equations.

$$f'' = \Delta(\sin A + \dot{\delta}\cos A)\,(\theta' - N_r s') \tag{18}$$

$$\theta'' + \frac{1}{2} f\theta' + N_b s'\theta' + N_t \theta'^2 - \xi S_T f' = 0 \tag{19}$$

$$s'' + \frac{1}{2} Lef s' + \frac{N_t}{N_b}\theta'' = 0 \tag{20}$$

The associated boundary conditions are

$$f = 0, \quad \theta = 1 - S_T\xi, \quad s = 1, \quad \text{at} \quad \eta = 0 \tag{21a}$$

$$f' = 1, \quad \theta \to 0, \quad s \to 0 \quad \text{as} \quad \eta \to \infty, \tag{21b}$$

For the second level of truncation we introduce $g = \frac{\partial f}{\partial \xi}$, $h = \frac{\partial \theta}{\partial \xi}$ and $k = \frac{\partial s}{\partial \xi}$ and recover the neglected terms at the first level of truncation. Thus the governing equations at the second level reduces to

$$f'' = \Delta(\sin A + \dot{\delta}\cos A)\,(\theta' - N_r s') \tag{22}$$

$$\theta'' + \frac{1}{2} f\theta' + N_b s'\theta' + N_t \theta'^2 = \xi\,(S_T f' + f'h - \theta' g) \tag{23}$$

$$s'' + \frac{1}{2} Lef s' + \frac{N_t}{N_b}\theta'' = Le\xi\,(f'k - s'g) \tag{24}$$

The associated boundary conditions are

$$f + 2\xi g = 0, \quad \theta = 1 - S_T\xi, \quad s = 1, \quad \text{at} \quad \eta = 0 \tag{25a}$$

$$f' = 1, \quad \theta \to 0, \quad s \to 0 \quad \text{as} \quad \eta \to \infty, \tag{25b}$$

At the third level of truncation we differenciate Eqns. (22) - (25) with respect to ξ and neglect the terms $\frac{\partial g}{\partial \xi}$, $\frac{\partial h}{\partial \xi}$ and $\frac{\partial k}{\partial \xi}$ to get the following system of equations

$$g'' = \Delta(\ddot{\delta}\cos A)\,(\theta' - N_r s') + \Delta(\sin A + \dot{\delta}\cos A)\,(h' - N_r k') \tag{26}$$

$$h'' + \frac{3}{2} g\theta' + \frac{1}{2} fh' + N_b(k'\theta' + s'h') + 2N_t\theta' h' - \xi(S_T g' + g'h - h'g) - S_T f' - f'h = 0 \tag{27}$$

$$k'' + \frac{3}{2} Legs' + \frac{1}{2} Lefk' + \frac{N_t}{N_b} h'' - Le\xi(g'k - k'g) - Lef'k = 0 \tag{28}$$

The associated boundary conditions are

$$g = 0, \quad h = -S_T, \quad k = 0, \quad \text{at} \quad \eta = 0 \tag{29a}$$

$$g' = 0, \quad h \to 0, \quad k \to 0 \quad \text{as} \quad \eta \to \infty, \tag{29b}$$

The set of differential equations (22) - (24) and (26) - (28) together with the boundary conditions (25) - (29) are solved using successive linearisation method([22–24]). Using this method the non linear boundary layer equations reduce to a system of linear differential equations. The Chebyshev pseudo spectral method is then used to transform the iterative sequence of linearized differential equations into a system of linear algebraic equations which are converted into a matrix system. In this method we assume that the independent variables $f(\eta)$, $\theta(\eta)$, $s(\eta)$, $g(\eta)$, $h(\eta)$ and $k(\eta)$ can be expressed as

$$f(\eta) = f_i(\eta) + \sum_{n=0}^{i-1} f_n(\eta), \quad \theta(\eta) = \theta_i(\eta) + \sum_{n=0}^{i-1} \theta_n(\eta), \quad s(\eta) = s_i(\eta) + \sum_{n=0}^{i-1} s_n(\eta) \tag{30}$$

$$g(\eta) = g_i(\eta) + \sum_{n=0}^{i-1} g_n(\eta), \quad h(\eta) = h_i(\eta) + \sum_{n=0}^{i-1} h_n(\eta), \quad k(\eta) = k_i(\eta) + \sum_{n=0}^{i-1} k_n(\eta)$$

where f_i, θ_i, s_i, g_i, h_i and k_i, $(i = 1, 2, 3, ...)$ are unknown functions and f_n, θ_n, s_n, g_n, h_n and k_n are the approximations which are obtained by recursively solving the linear part of the equation system that results from substituting (30) in (22)-(29).

The initial guesses $f_0(\eta)$, $\theta_0(\eta)$, $s_0(\eta)$, $g_0(\eta)$, $h_0(\eta)$, and $k_0(\eta)$ are taken as

$$\begin{aligned} f_0(\eta) = 1 + \eta - e^{-\eta}, \quad \theta_0(\eta) = (1 - S_T\xi)e^{-\eta}, \quad s_0(\eta) = e^{-\eta} \\ g_0(\eta) = 1 - e^{-\eta}, \quad h_0(\eta) = -S_T e^{-\eta}, \quad k_0(\eta) = \eta e^{-\eta} \end{aligned} \tag{31}$$

These initial approximations are chosen such that they satisfy the boundary conditions (25) and (29). The subsequent solutions f_i, θ_i, s_i, g_i, h_i, and k_i ,$i \geq 1$ are obtained by successively solving the linearized form of the equations which are obtained by substituting Eq.(30) in the governing equations.

The approximate solutions for $f(\eta)$, $\theta(\eta)$, $s(\eta)$, $g(\eta)$, $h(\eta)$ and $k(\eta)$ are then obtained as

$$\begin{aligned} f(\eta) \approx \sum_{m=0}^{M} f_m(\eta), \quad \theta(\eta) \approx \sum_{m=0}^{M} \theta_m(\eta), \quad s(\eta) \approx \sum_{m=0}^{M} s_m(\eta) \\ g(\eta) \approx \sum_{m=0}^{M} g_m(\eta), \quad h(\eta) \approx \sum_{m=0}^{M} h_m(\eta), \quad k(\eta) \approx \sum_{m=0}^{M} k_m(\eta) \end{aligned} \tag{32}$$

where M is the order of SLM approximation. The linearized equations were solved using the Chebyshev spectral collocation method ([25]). The unknown functions are approximated by the Chebyshev interpolating polynomials in such a way that they are collocated at the Gauss-Lobatto points defined as

$$\xi_j = \cos\frac{\pi j}{N}, \quad j = 0, 1, 2, ..., N \tag{33}$$

where N is the number of collocation points used. The physical region $[0, \infty)$ is transformed into the region [-1, 1] using the domain truncation technique in which the problem is solved on the interval [0, L] instead of $[0, \infty)$. This leads to the mapping

$$\frac{\eta}{L} = \frac{\xi + 1}{2}, \quad -1 \leq \xi \leq 1 \tag{34}$$

where L is a scaling parameter used to invoke the boundary condition at infinity. The functions f_i, θ_i, s_i, g_i, h_i and k_i are approximated at the collocation points by

$$\begin{aligned} f_i(\xi) = \sum_{k=0}^{N} f_i(\xi_k)T_k(\xi_j), \ \theta_i(\xi) = \sum_{k=0}^{N} \theta_i(\xi_k)T_k(\xi_j), \ s_i(\xi) = \sum_{k=0}^{N} s_i(\xi_k)T_k(\xi_j), \\ g_i(\xi) = \sum_{k=0}^{N} g_i(\xi_k)T_k(\xi_j), \ h_i(\xi) = \sum_{k=0}^{N} h_i(\xi_k)T_k(\xi_j), \ k_i(\xi) = \sum_{k=0}^{N} k_i(\xi_k)T_k(\xi_j), \\ j = 0, 1, 2, ..., N \end{aligned} \tag{35}$$

where T_k is the k^{th} Chebyshev polynomial defined by

$$T_k(\xi) = \cos[k\cos^{-1}\xi] \tag{36}$$

The derivatives of the variables at the collocation points are represented as

$$\begin{aligned} \frac{d^a f_i}{d\eta^a} = \sum_{k=0}^{N} \mathbf{D}_{kj}^a f_i(\xi_k), \quad \frac{d^a \theta_i}{d\eta^a} = \sum_{k=0}^{N} \mathbf{D}_{kj}^a \theta_i(\xi_k), \quad \frac{d^a s_i}{d\eta^a} = \sum_{k=0}^{N} \mathbf{D}_{kj}^a s_i(\xi_k) \\ \frac{d^a g_i}{d\eta^a} = \sum_{k=0}^{N} \mathbf{D}_{kj}^a g_i(\xi_k), \quad \frac{d^a h_i}{d\eta^a} = \sum_{k=0}^{N} \mathbf{D}_{kj}^a h_i(\xi_k), \quad \frac{d^a k_i}{d\eta^a} = \sum_{k=0}^{N} \mathbf{D}_{kj}^a k_i(\xi_k) \\ j = 0, 1, 2, ..., N. \end{aligned} \tag{37}$$

where a is the order of differentiation and $\mathbf{D} = \frac{2}{L}\mathcal{D}$ with $\mathcal{D}$ being the Chebyshev spectral differentiation matrix. Substituting Eqs.(34)-(37) into linearized form of equations leads to the matrix equation

$$\mathbf{A}_{i-1}\mathbf{X}_i = \mathbf{R}_{i-1}, \tag{38}$$

In Eq.(38), $\mathbf{A}_{i-1}$ is a (6N + 6)×(6N + 6) square matrix and $\mathbf{X}_i$ and $\mathbf{R}_{i-1}$ are (6N + 6)×1 column vectors defined by

$$\mathbf{A}_{i-1} = \begin{bmatrix} A_{11} & A_{12} & A_{13} & A_{14} & A_{15} & A_{16} \\ A_{21} & A_{22} & A_{23} & A_{24} & A_{25} & A_{26} \\ A_{31} & A_{32} & A_{33} & A_{34} & A_{35} & A_{36} \\ A_{41} & A_{42} & A_{43} & A_{44} & A_{45} & A_{46} \\ A_{51} & A_{52} & A_{53} & A_{54} & A_{55} & A_{56} \\ A_{61} & A_{62} & A_{63} & A_{64} & A_{65} & A_{66} \end{bmatrix}, \quad \mathbf{X}_i = \begin{bmatrix} \mathbf{F}_i \\ \mathbf{\Theta_i} \\ \mathbf{\Phi_i} \\ \mathbf{G}_i \\ \mathbf{H}_i \\ \mathbf{K}_i \end{bmatrix}, \quad \mathbf{R}_{i-1} = \begin{bmatrix} \mathbf{r}_{1,i-1} \\ \mathbf{r}_{2,i-1} \\ \mathbf{r}_{3,i-1} \\ \mathbf{r}_{4,i-1} \\ \mathbf{r}_{5,i-1} \\ \mathbf{r}_{6,i-1} \end{bmatrix} \tag{39}$$

where

$$\left.\begin{array}{l} \mathbf{F}_i = [f_i(\xi_0), f_i(\xi_1), \cdots, f_i(\xi_{N-1}), f_i(\xi_N)]^T, \\ \mathbf{\Theta_i} = [\theta_i(\xi_0), \theta_i(\xi_1), \cdots, \theta_i(\xi_{N-1}), \theta_i(\xi_N)]^T, \\ \mathbf{\Phi_i} = [s_i(\xi_0), s_i(\xi_1), \cdots, s_i(\xi_{N-1}), s_i(\xi_N)]^T, \\ \mathbf{G}_i = [g_i(\xi_0), g_i(\xi_1), \cdots, g_i(\xi_{N-1}), g_i(\xi_N)]^T, \\ \mathbf{H}_i = [h_i(\xi_0), h_i(\xi_1), \cdots, h_i(\xi_{N-1}), h_i(\xi_N)]^T, \\ \mathbf{K}_i = [k_i(\xi_0), k_i(\xi_1), \cdots, k_i(\xi_{N-1}), k_i(\xi_N)]^T, \\ \mathbf{r}_{j,i-1} = [r_{j,i-1}(\xi_0), r_{j,i-1}(\xi_1), \cdots, r_{j,i-1}(\xi_{N-1}), r_{j,i-1}(\xi_N)]^T, j = 1,2,3,4,5,6 \\ A_{11} = \mathbf{D}^2, \quad A_{12} = a_{1,i-1}\mathbf{D}, \quad A_{13} = a_{2,i-1}\mathbf{D}, \quad A_{14} = \mathbf{0}, \quad A_{15} = \mathbf{0}, \quad A_{16} = \mathbf{0} \\ A_{21} = b_{2,i-1}\mathbf{D} + b_{3,i-1}I, \quad A_{22} = \mathbf{D}^2 + b_{1,i-1}\mathbf{D}, \quad A_{23} = b_{4,i-1}\mathbf{D} \\ A_{24} = b_{5,i-1}I, \quad A_{25} = b_{6,i-1}I, \quad A_{26} = \mathbf{0} \\ A_{31} = c_{2,i-1}\mathbf{D} + c_{3,i-1}I, \quad A_{32} = c_{4,i-1}\mathbf{D}^2, \quad A_{33} = \mathbf{D}^2 + c_{1,i-1}\mathbf{D} \\ A_{34} = c_{5,i-1}I, \quad A_{35} = \mathbf{0}, \quad A_{36} = c_{6,i-1}I \\ A_{41} = \mathbf{0}, \quad A_{42} = d_{1,i-1}\mathbf{D}, \quad A_{43} = d_{2,i-1}\mathbf{D} \\ A_{44} = \mathbf{D}^2, \quad A_{45} = d_{3,i-1}\mathbf{D}, \quad A_{46} = d_{4,i-1}\mathbf{D} \\ A_{51} = l_{3,i-1}\mathbf{D} + l_{4,i-1}I, \quad A_{52} = l_{5,i-1}\mathbf{D}, \quad A_{53} = l_{6,i-1}\mathbf{D} \\ A_{54} = l_{7,i-1}\mathbf{D} + l_{8,i-1}I, \quad A_{55} = \mathbf{D}^2 + l_{1,i-1}\mathbf{D} + l_{2,i-1}I, \quad A_{56} = l_{9,i-1}\mathbf{D} \\ A_{61} = m_{3,i-1}\mathbf{D} + m_{4,i-1}I, \quad A_{62} = 0, \quad A_{63} = m_{5,i-1}\mathbf{D} \\ A_{64} = m_{6,i-1}\mathbf{D} + m_{7,i-1}I, \quad A_{65} = m_{8,i-1}\mathbf{D}^2, \quad A_{66} = \mathbf{D}^2 + m_{1,i-1}\mathbf{D} + m_{2,i-1}I \end{array}\right\} \tag{40}$$

Here $a_{k,i-1}$, $b_{k,i-1}$, $c_{k,i-1}$,$d_{k,i-1}$, $l_{k,i-1}$, $m_{k,i-1}$ are diagonal matrices of size (N+1)×(N+1) and I is an identity matrix of size (N +1)×(N +1). After modifying the matrix system (38) to incorporate boundary conditions, the solution is obtained as

$$\mathbf{X}_i = \mathbf{A}_{i-1}^{-1}\mathbf{R}_{i-1} \tag{41}$$

4 Results and Discussion

Numerical solutions for the dimensionless velocity, temperature and nanoparticle volume fraction functions and heat and nanoparticle mass transfer rates for aiding and opposing flows have been computed and displayed graphically in Figs. 2 - 3. The effects of thermal stratification S_T, angle of inclination A, Brownian motion parameter N_b, thermoporesis parameter N_t and amplitude a of the wavy surface have been discussed.

Table. 1 shows the comparison of the results of $-\theta'(0)$ for both aiding and opposing flows of the present paper for fixed values of $A = \frac{\pi}{2}$, $a = 0$, $\xi = 0$, $N_r = 0$, $N_t = 0$, $N_b = 0$, $Le = 0$, $F_c = 0$, $R = 0$ with the results obtained by Cheng [26]. It is observed that these two results are in excellent agreement.

Figures 4 - 5 illustrate the effect of thermal stratification on velocity, temperature and nanoparticle volume fraction distributions for both aiding and opposing flows respectively. It is noticed from Figure 4 that increasing the thermal stratification parameter S_T reduces the velocity for aiding flow. This is because thermal stratification reduces the effective convective potential between the heated plate and ambient fluid in the medium. Hence, the thermal stratification effect reduces velocity in the boundary layer. The temperature of the fluid decreases with an increase in the value of thermal stratification parameter. When thermal stratification is taken into consideration, the effective temperature difference between the plate and the ambient fluid will decrease; therefore, the thermal boundary layer is thickened and the temperature

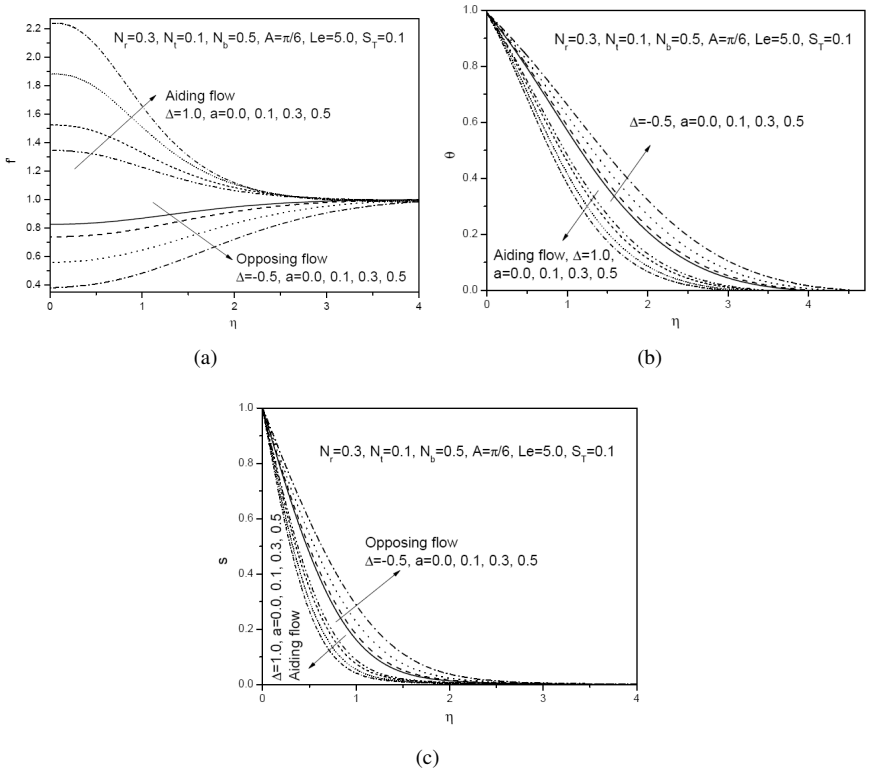

Figure 2: Variation of (a) Velocity, (b) Temperature, (c) Nanoparticle volume fraction Profiles with the wave amplitude (a) for both Aiding and Opposing flows.

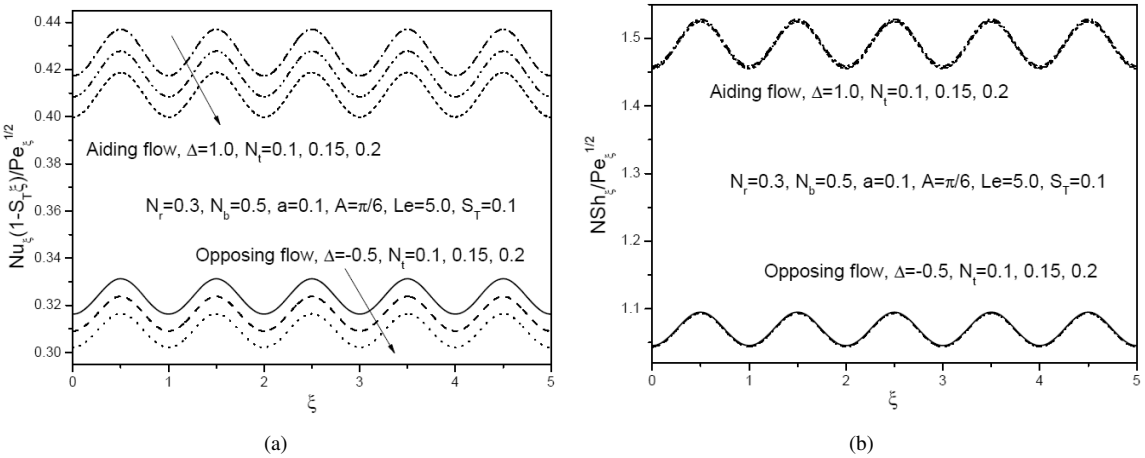

Figure 3: Effect of the thermoporesis parameter (N_t) on the heat and nanoparticle mass transfer rates.

Table 1: Comparison of values of $-\theta'(0)$ for Aiding and Opposing flow by the present method and Cheng [26] for fixed values of for $A = \frac{\pi}{2}$, $a = 0$, $\xi = 0$, $N_r = 0$, $N_t = 0$, $N_b = 0$, $Le = 0$.

Aiding Flow			Opposing Flow		
Δ	Cheng [26]	Present	Δ	Cheng [26]	Present
0	0.5641	0.56415775	-0.2	0.5269	0.52691089
0.5	0.6473	0.64736510	-0.4	0.4865	0.48653284
1	0.7205	0.72055401	-0.6	0.442	0.44202064
3	0.9574	0.95744512	-0.8	0.3916	0.39166292
10	1.516	1.51623967	-1.0	0.332	0.33202116
20	2.066	2.066			

is reduced. The nanoparticle volume fraction of the fluid flow increases with increase in the value of thermal stratification parameter for aiding flow. It is observed from Figure 5 that the velocity increases and temperature and nanoparticle volume fraction decreases as thermal stratification parameter increases in the case of opposing flow.

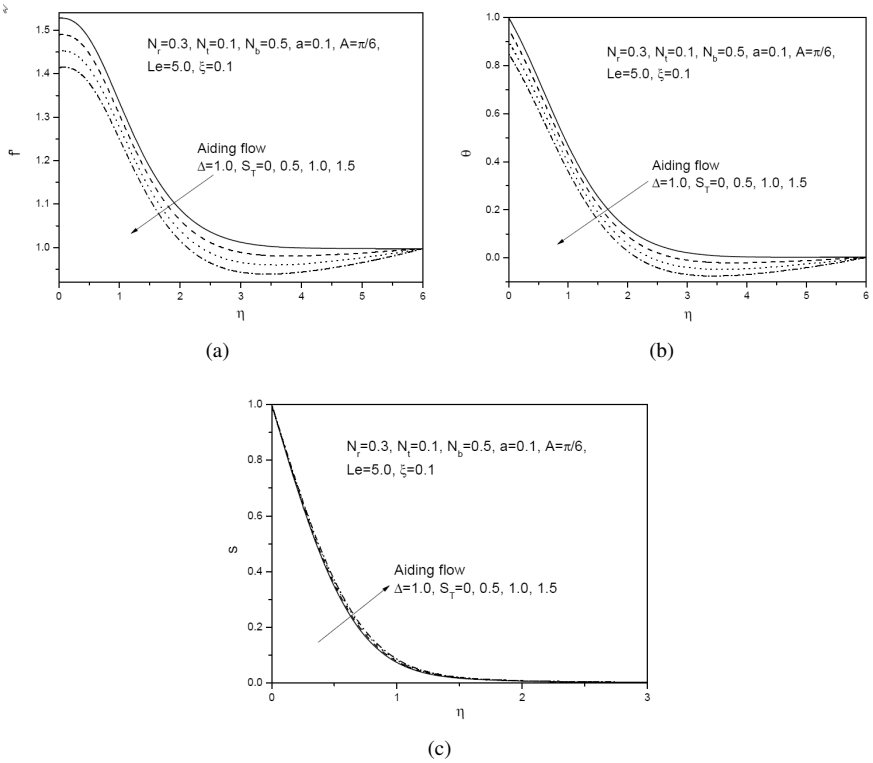

Figure 4: Variation of (a) Velocity, (b) Temperature (c) Nanoparticle volume fraction profiles with Thermal stratification parameter (S_T) for Aiding flow.

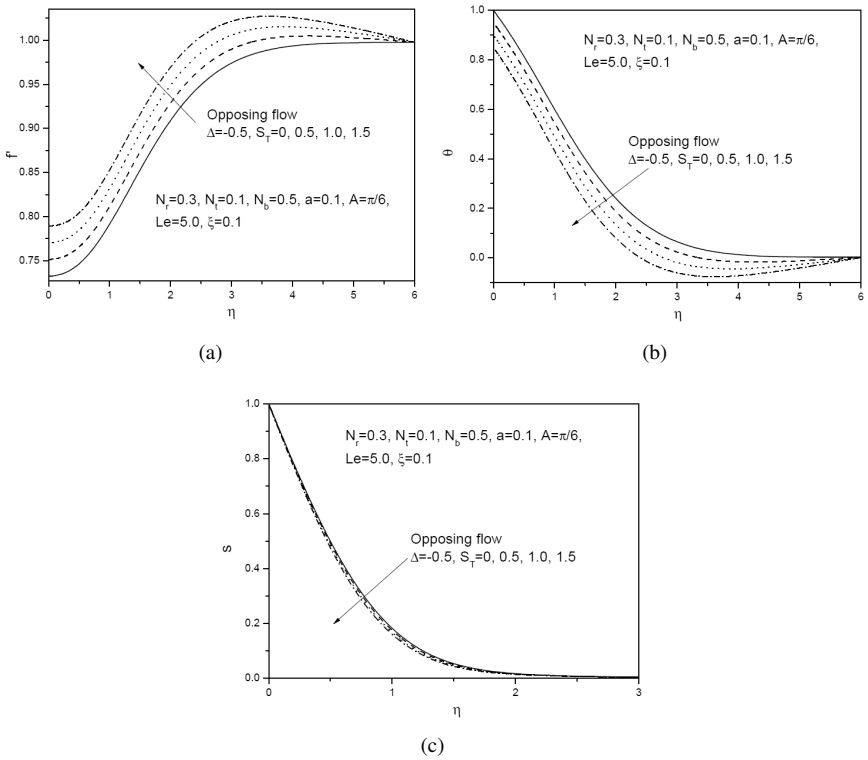

Figure 5: Variation of (a) Velocity, (b) Temperature (c) Nanoparticle volume fraction profiles with Thermal stratification parameter (S_T) for Opposing flow.

The effect of amplitude of the wavy surface a on the velocity, temperature and nanoparticle volume fraction for both aiding and opposing flows respectively are plotted in Figure 2. It is observed that as a increases, velocity increases but the temperature and nanoparticle volume fraction decreases for aiding flow whereas the velocity decreases and the temperature and nanoparticle volume fraction of the fluid flow increases in the case of opposing flow.

Figure 6 displays the effect of angle of inclination A on the velocity, temperature and nanoparticle volume fraction for both aiding and opposing flows respectively. The equations for the limiting cases of the horizontal and vertical plates are recovered from the transformed equations by setting $A = 0^o$ and $A = 90^o$, respectively. It is noted from Figure 6 that as A increases, the velocity increases near the plate but the temperature and nanoparticle volume fraction decrease within the boundary layer region for the aiding flow whereas velocity reduces but the temperature and nanoparticle volume fraction enhances for opposing flow. When the surface is vertical, the smallest temperature and nanoparticle volume fraction distributions are observed, whereas they are largest for the horizontal surface.

The effect of the wave amplitude on the local Nusselt number $Nu_\xi(1 - S_T\xi)/{Pe_\xi}^{1/2}$ and nanoparticle Sherwood number $NSh_\xi/{Pe_\xi}^{1/2}$ is plotted in Figure 7. This figure reveals that an enhancement in wavy amplitude decreases the local heat and nanoparticle mass transfer rates for both aiding and opposing flows. In general, we conclude that the surface becomes more roughened for increasing values of amplitude of the wavy surface. The variation of heat and nanoparticle mass transfer rates for various values of the angle of inclination A is displayed in Figure 8. This figure shows that increasing the angle of inclination increases the buoyancy force and assist the flow, leading to an increase in the heat and nanoparticle mass transfer rates in the case of aiding flow where as a reverse tend is seen in the case of opposing flow. The maximum values of the dimensionless heat and nanoparticle mass transfer rates are observed when the surface is vertical.

The effect of Brownian motion parameter N_b on the heat and nanoparticle mass transfer rates is plotted in Figure 9. It is observed that the local heat transfer rate decreases with increase in the Browinian motion parameter N_b whereas the nanoparticle mass transfer rate increases with an increase in the value of Brownian motion parameter N_b for aiding flow where as a reverse pattern is observed in the case of apposing flow.

Figure 3 displays the effect of local Nusselt $Nu_\xi(1-S_T\xi)/{Pe_\xi}^{1/2}$ and nanoparticle Sherwood number $NSh_\xi/{Pe_\xi}^{1/2}$ for both aiding and opposing flows along the wavy surface on the thermophoresis parameter N_t. It is seen that the heat

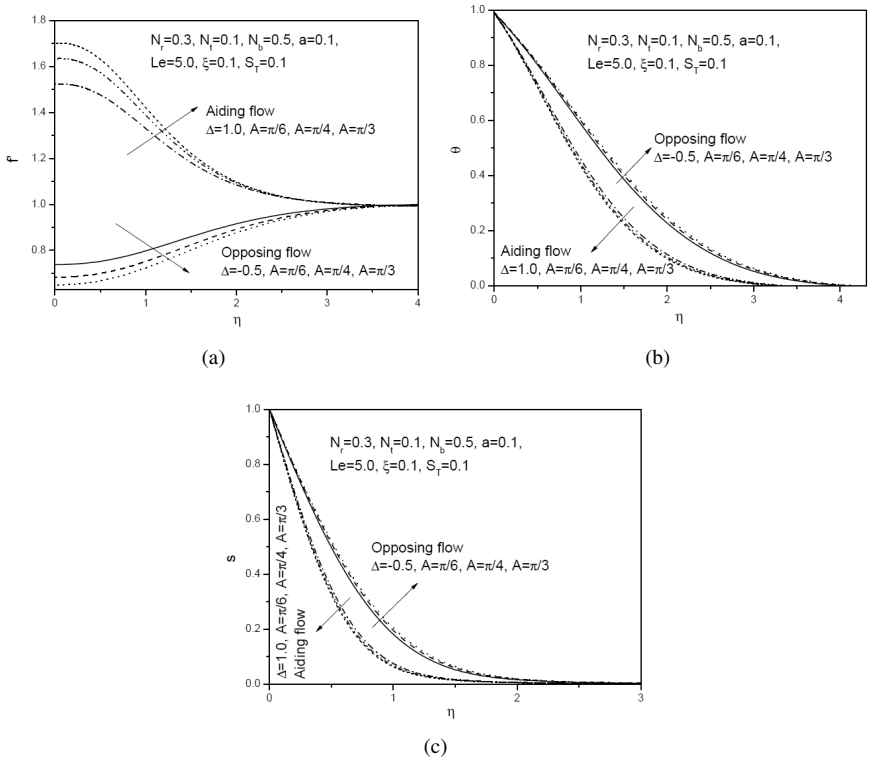

Figure 6: Variation of (a) Velocity, (b) Temperature, (c) Nanoparticle volume fraction profiles with Angle of inclination $(A)$for both Aiding and Opposing flows.

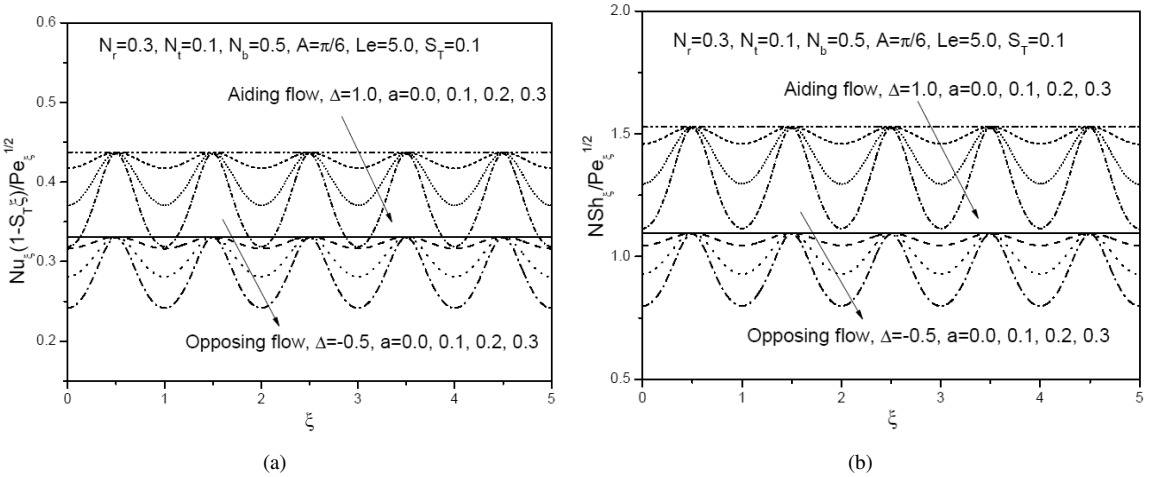

Figure 7: Effect of the wave amplitude a on the heat and nanoparticle mass transfer rates

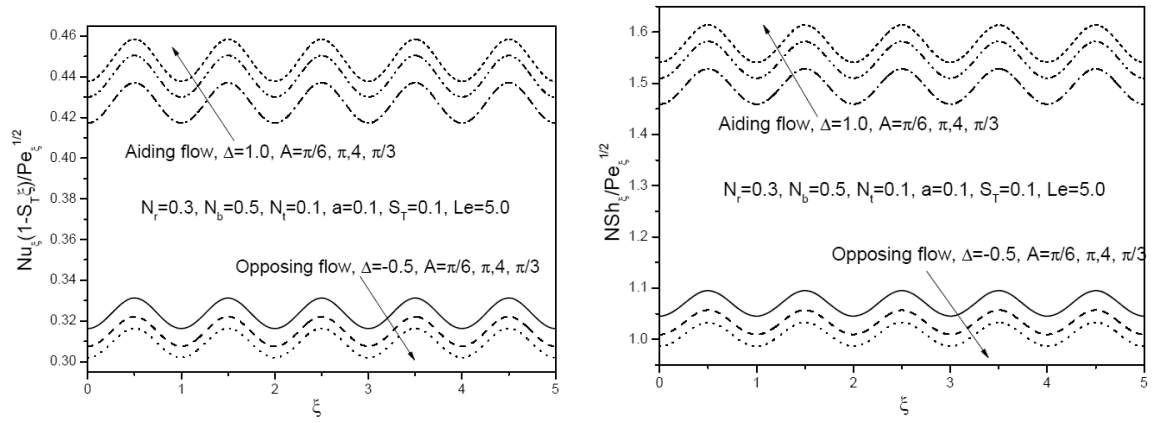

Figure 8: Effect of the Angle of inclination (A) on the heat and nanoparticle mass transfer rates.

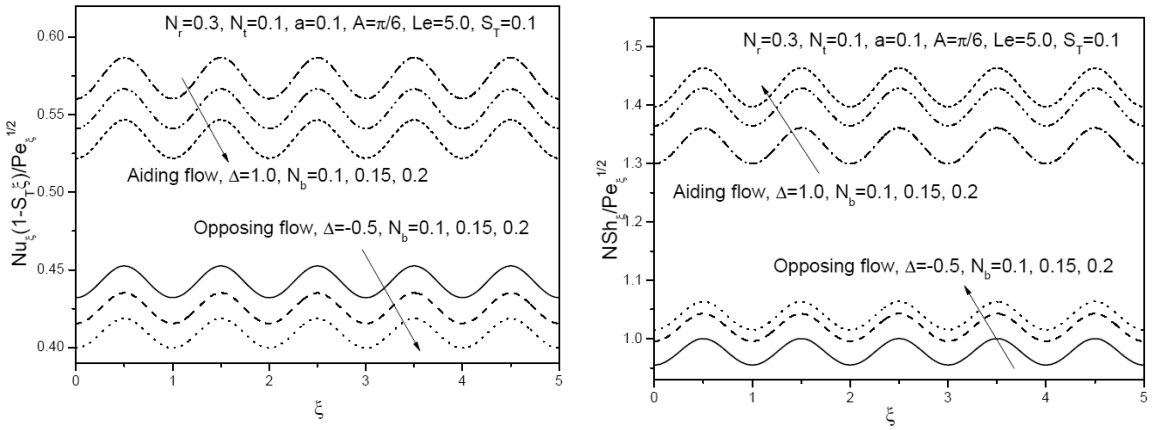

Figure 9: Effect of the Brownian motion parameter (N_b) on the heat and nanoparticle mass transfer rates.

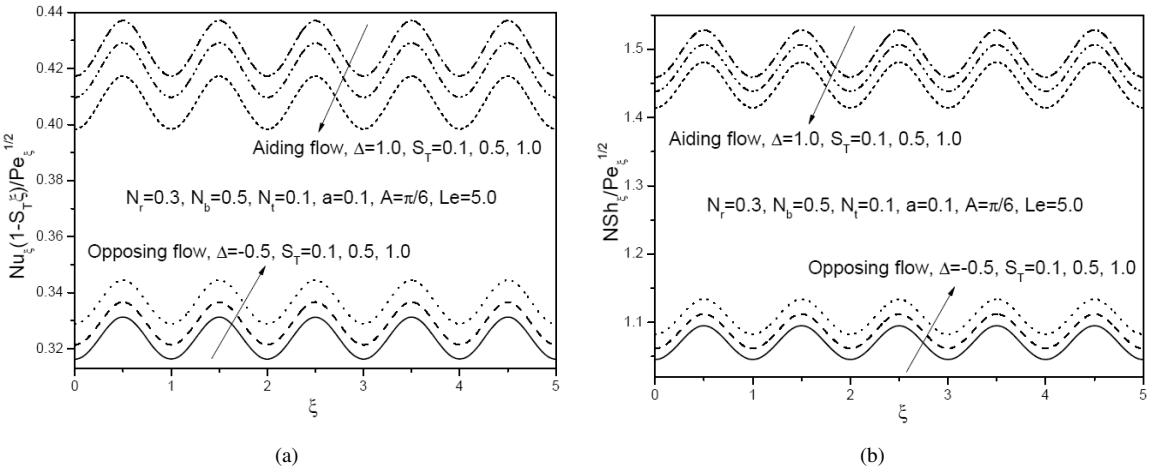

Figure 10: Effect of the thermal stratification parameter (S_T) on the heat and nanoparticle mass transfer rates.

transfer rate decreases with increase in the value of thermophoresis parameter N_t for both aiding and opposing flows and a negligible effect of thermophoresis Parameter N_t on nanoparticle mass transfer is also observed.

Brownian motion is proportional to the volumetric fraction of nanoparticles in the direction from high to low concentration, whereas the thermophoresis is proportional to the temperature gradient from hot to cold. Hence, we conclude that the effect of the combination of Brownian motion and thermophoresis is to reduce the value of Nusselt number.

The streamwise distribution of the local Nusselt $Nu_\xi(1-S_T\xi)/{Pe_\xi}^{1/2}$ and nanoparticle Sherwood numbers $NSh_\xi/{Pe_\xi}^{1/2}$ for different values of thermal stratification parameter S_T is displayed in Figure 3. It is observed that both the heat and nanoparticle mass transfer rates decreases with increasing the thermal stratification parameter S_T for aiding flow whereas a reverse trend is seen in the case of opposing flow.

5 Conclusions

Mixed convection heat and mass transfer over an inclined wavy surface embedded in a thermally stratified porous medium saturated with nanofluid is analyzed. Numerical solutions were obtained for different values of thermal stratification, Brownian motion parameter, thermophoresis parameter, amplitude and angle of inclination of the wavy surface. The following conclusions are drawn

- Increasing the thermal stratification parameter reduce the velocity, temperature, local heat and nanoparticle mass transfer rates but enhances the nanoparticle volume fraction of the fluid for aiding flow, whereas the velocity, local heat and mass transfer rates increase and the temperature and nanoparticle volume fraction decrease in the case of opposing flow.
- The wave amplitude a significantly effects the velocity, temperature, nanoparticle volume fraction, local heat transfer and nanoparticle mass transfer coefficients for both aiding and opposing flows.
- The influence of the angle of inclination A of the wavy surface to the horizontal is to enhance the velocity, local heat transfer and nanoparticle mass transfer rates, but to reduce the temperature and nanoparticle volume fraction of the fluid flow for aiding flow and to reduce the velocity, local heat and nanoparticle mass transfer rates in the case of opposing flow.

References

[1] S. U. S. Choi, and J. A. Eastman, Enhancing thermal conductivity of fluids with Nanoparticles, Developments and applications of Non-Newtonian flows,*ASME FED* 231, 99-105, (1995).

[2] Y. Xuan, and Q. Li, Investigation on convective heat transfer and flow features of nanofluids, *J. Heat Transfer*, 125, 151-155, (2003).

[3] Y. Ding, H., D. Alias, Wen and R. A. Williams, Heat transfer of aqueous suspensions of carbon nanotubes (CNT nanofluids), *Int. J. Heat Mass Transfer*, 49, 240-250, (2006).

[4] P. Rana, R. Bhargava and O. A. Beg, Numerical solution for mixed convection boundary layer flow of a nanofluid along an inclined plate embedded in a porous medium, *Computer and Mathematics with Applications*, 64, 2816-2832, (2012).

[5] S. K. Das, S. U. S. Choi, W. Yu and T. Pradeep, Nanofluids: Science and Technology, Wiley Interscience, New Jersey (2007).

[6] S. Kakac, and A. Pramuanjaroenkij, Review of convective heat transfer enhancement with nano fluids, *Int. J. Heat Mass Transfer*, 52, 3187-3196, (2009).

[7] P. Gianluca, P. Samuel and M. Sen, Nanofluids and their properties, *Appl. Mech. Reviews*, 64, 030803 (2011)

[8] D. A. Nield and A. Bejan, Convection in Porous Media, 4th ed., Springer, New York (2013).

[9] S. Mirmasoumi and Behzadmehr, Effect of nanoparticles mean diameter on mixed convection heat transfer of a nanofluid in a horizontal tube, *Int. J. Heat and Fluid Flow*, 29, 557-566, (2008).

[10] C. C. Cho, C.L. Chen, and C.K. Chen, Mixed convection heat transfer performance of water-based nanofluids in lid-driven cavity with wavy surfaces, *Int. J. Thermal Sciences*, 68, 181-190, (2013).

[11] A. Rasekh and D. D. Ganji, Analytic approximate solutions of mixed convection about an inclined flat plate embedded in a porous medium filled with nanofluid, *Int. J. for computational methods in Engineering Science and Mechanics*, 1-34 (2013).

[12] A. Ishak, R. Nazar, and I. Pop, Mixed convection boundary layer flow over a vertical surface embedded in a thermally stratified porous medium, *Physics Letters A*, 372, 2355 -2358, (2008).

[13] V. J. Bansod and R. K. Jadhav, Effect of double stratification on mixed convection heat and mass transfer from a vertical surface in a fluid saturated porous medium, *Heat Transfer - Asian Research*, 39, 378-395, (2010).

[14] W. Ibrahim and O. D. Makinde, The effect of double stratification on boundary layer flow and heat transfer of nanofluid over a vertical plate, *Computers and Fluids*, 86, 433-441, (2013).

[15] A. A. M. Mahmoud and S. E. Waheed, Mixed convection flow of a micropolar fluid past a vertical stretching surface in a thermally stratified porous medium with thermal radiation, *Journal of Mechanics*, 29, 461-470, (2013).

[16] M. H. M. Yasin, N. M. Arifin, R. Nazar, F. Ismail, and I. Pop, Mixed convection boundary layer ow embedded in a thermally stratified porous medium saturated by a nanofluid, *Advances in Mechanical Engineering*, 2013, 1-8, (2013).

[17] S. A. Shezad, A. Qasim, A. Alsaedi, T. Hayat and M. S. Alhothuali, Combined thermal stratified and thermal radiation effects in mixed convection flow of a thixotropic fluid, *Eur. Phys. J. Plus*, 128, 1-10, (2013).

[18] D. Srinivasacharya and O. Surender, Mixed convection boundary layer flow of a nanofluid past a vertical plate in a doubly stratified porous medium, *Journal of Comput. Theor. Nanosci.*, 11, 1853-1862, (2014).

[19] A. M. Rashad, S. Abbasbandy and A. J. Chamkha, Mixed convection flow of a micropolar fluid over a continuously moving vertical surface immersed in a thermally and solutally stratified medium with chemical reaction, *J. Taiwan Inst Chem Eng.*, 1-7, (2014).

[20] W. J. Minkowycz and E. M. Sparrow, Local non-similar solution for natural convection on a vertical cylinder, *ASME J. Heat Transfer* 96, 178-183, (1974).

[21] E. M. Sparrow and H. S. Yu, Local non-similar solution for natural convection on a vertical cylinder, *ASME J. Heat Transfer*, 93, 328-332, (1971).

[22] S. S. Motsa and S. Shateyi, Successive linearisation solution of free convection non-Darcy flow with heat and mass transfer, *Advanced topics in mass transfer*, 19, 425-438, (2006).

[23] Z. G. Makukula, P. Sibanda and S. S. Motsa, A novel numerical technique for two dimensional laminar flow between two moving porous walls, *Mathematical problems in Engineering*, 2010, 1-15, (2010).

[24] F. G. Awad, P. Sibanda, S. S. Motsa, O. D. Makinde, Convection from an inverted cone in a porous medium with cross-diffusion effects, *Computers and Mathematics with Applications*, 61, 1431-1441, (2011).

[25] C. Canuto, M. Y. Hussaini, A. Quarteroni and T. A. Zang, Spectral Methods Fundamentals in Single Domains, *Springer Verlag*, (2006).

[26] P. Cheng, Combined free and forced convection flow about inclined surfaces in porous media, *Int. J. Heat Mass Transfer*,20, 807-814, (1977).